

Study of $e^+e^- \rightarrow p\bar{p}$ in the vicinity of $\psi(3770)$

M. Ablikim¹, M. N. Achasov^{8,a}, X. C. Ai¹, O. Albayrak⁴, M. Albrecht³, D. J. Ambrose⁴¹, F. F. An¹, Q. An⁴², J. Z. Bai¹, R. Baldini Ferrolli^{19A}, Y. Ban²⁸, J. V. Bennett¹⁸, M. Bertani^{19A}, J. M. Bian⁴⁰, E. Boger^{21,e}, O. Bondarenko²², I. Boyko²¹, S. Braun³⁷, R. A. Briere⁴, H. Cai⁴⁷, X. Cai¹, O. Cakir^{36A}, A. Calcaterra^{19A}, G. F. Cao¹, S. A. Cetin^{36B}, J. F. Chang¹, G. Chelkov^{21,b}, G. Chen¹, H. S. Chen¹, J. C. Chen¹, M. L. Chen¹, S. J. Chen²⁶, X. Chen¹, X. R. Chen²³, Y. B. Chen¹, H. P. Cheng¹⁶, X. K. Chu²⁸, Y. P. Chu¹, D. Cronin-Hennessy⁴⁰, H. L. Dai¹, J. P. Dai¹, D. Dedovich²¹, Z. Y. Deng¹, A. Denig²⁰, I. Denysenko²¹, M. Destefanis^{45A,45C}, W. M. Ding³⁰, Y. Ding²⁴, C. Dong²⁷, J. Dong¹, L. Y. Dong¹, M. Y. Dong¹, S. X. Du⁴⁹, J. Z. Fan³⁵, J. Fang¹, S. S. Fang¹, Y. Fang¹, L. Fava^{45B,45C}, C. Q. Feng⁴², C. D. Fu¹, O. Fuks^{21,e}, Q. Gao¹, Y. Gao³⁵, C. Geng⁴², K. Goetzen⁹, W. X. Gong¹, W. Gradl²⁰, M. Greco^{45A,45C}, M. H. Gu¹, Y. T. Gu¹¹, Y. H. Guan¹, L. B. Guo²⁵, T. Guo²⁵, Y. P. Guo²⁰, Y. L. Han¹, F. A. Harris³⁹, K. L. He¹, M. He¹, Z. Y. He²⁷, T. Held³, Y. K. Heng¹, Z. L. Hou¹, C. Hu²⁵, H. M. Hu¹, J. F. Hu³⁷, T. Hu¹, G. M. Huang⁵, G. S. Huang⁴², H. P. Huang⁴⁷, J. S. Huang¹⁴, L. Huang¹, X. T. Huang³⁰, Y. Huang²⁶, T. Hussain⁴⁴, C. S. Ji⁴², Q. Ji¹, Q. P. Ji²⁷, X. B. Ji¹, X. L. Ji¹, L. L. Jiang¹, L. W. Jiang⁴⁷, X. S. Jiang¹, J. B. Jiao³⁰, Z. Jiao¹⁶, D. P. Jin¹, S. Jin¹, T. Johansson⁴⁶, N. Kalantar-Nayestanaki²², X. L. Kang¹, X. S. Kang²⁷, M. Kavatsyuk²², B. Kloss²⁰, B. Kopf³, M. Kornicer³⁹, W. Kühn³⁷, A. Kupsc⁴⁶, W. Lai¹, J. S. Lange³⁷, M. Lara¹⁸, P. Larin¹³, M. Leyhe³, C. H. Li¹, Cheng Li⁴², Cui Li⁴², D. Li¹⁷, D. M. Li⁴⁹, F. Li¹, G. Li¹, H. B. Li¹, J. C. Li¹, K. Li¹², K. Li³⁰, Lei Li¹, P. R. Li³⁸, Q. J. Li¹, T. Li³⁰, W. D. Li¹, W. G. Li¹, X. L. Li³⁰, X. N. Li¹, X. Q. Li²⁷, Z. B. Li³⁴, H. Liang⁴², Y. F. Liang³², Y. T. Liang³⁷, D. X. Lin¹³, B. J. Liu¹, C. L. Liu⁴, C. X. Liu¹, F. H. Liu³¹, Fang Liu¹, Feng Liu⁵, H. B. Liu¹¹, H. H. Liu¹⁵, H. M. Liu¹, J. Liu¹, J. P. Liu⁴⁷, K. Liu³⁵, K. Y. Liu²⁴, P. L. Liu³⁰, Q. Liu³⁸, S. B. Liu⁴², X. Liu²³, Y. B. Liu²⁷, Z. A. Liu¹, Zhiqiang Liu¹, Zhiqing Liu²⁰, H. Loehner²², X. C. Lou^{1,c}, G. R. Lu¹⁴, H. J. Lu¹⁶, H. L. Lu¹, J. G. Lu¹, X. R. Lu³⁸, Y. Lu¹, Y. P. Lu¹, C. L. Luo²⁵, M. X. Luo⁴⁸, T. Luo³⁹, X. L. Luo¹, M. Lv¹, F. C. Ma²⁴, H. L. Ma¹, Q. M. Ma¹, S. Ma¹, T. Ma¹, X. Y. Ma¹, F. E. Maas¹³, M. Maggiora^{45A,45C}, Q. A. Malik⁴⁴, Y. J. Mao²⁸, Z. P. Mao¹, J. G. Messchendorp²², J. Min¹, T. J. Min¹, R. E. Mitchell¹⁸, X. H. Mo¹, Y. J. Mo⁵, H. Moeini²², C. Morales Morales¹³, K. Moriya¹⁸, N. Yu. Muchnoi^{8,a}, H. Muramatsu⁴⁰, Y. Nefedov²¹, F. Nerling¹³, I. B. Nikolaev^{8,a}, Z. Ning¹, S. Nisar⁷, X. Y. Niu¹, S. L. Olsen²⁹, Q. Ouyang¹, S. Pacetti^{19B}, M. Pelizaeus³, H. P. Peng⁴², K. Peters⁹, J. L. Ping²⁵, R. G. Ping¹, R. Poling⁴⁰, M. Qi²⁶, S. Qian¹, C. F. Qiao³⁸, L. Q. Qin³⁰, N. Qin⁴⁷, X. S. Qin¹, Y. Qin²⁸, Z. H. Qin¹, J. F. Qiu¹, K. H. Rashid⁴⁴, C. F. Redmer²⁰, M. Ripka²⁰, G. Rong¹, X. D. Ruan¹¹, A. Sarantsev^{21,d}, K. Schoenning⁴⁶, S. Schumann²⁰, W. Shan²⁸, M. Shao⁴², C. P. Shen², X. Y. Shen¹, H. Y. Sheng¹, M. R. Shepherd¹⁸, W. M. Song¹, X. Y. Song¹, S. Spataro^{45A,45C}, B. Spruck³⁷, G. X. Sun¹, J. F. Sun¹⁴, S. S. Sun¹, Y. J. Sun⁴², Y. Z. Sun¹, Z. J. Sun¹, Z. T. Sun⁴², C. J. Tang³², X. Tang¹, I. Tapan^{36C}, E. H. Thorndike⁴¹, D. Toth⁴⁰, M. Ullrich³⁷, I. Uman^{36B}, G. S. Varner³⁹, B. Wang²⁷, D. Wang²⁸, D. Y. Wang²⁸, K. Wang¹, L. L. Wang¹, L. S. Wang¹, M. Wang³⁰, P. Wang¹, P. L. Wang¹, Q. J. Wang¹, S. G. Wang²⁸, W. Wang¹, X. F. Wang³⁵, Y. D. Wang^{19A}, Y. F. Wang¹, Y. Q. Wang²⁰, Z. Wang¹, Z. G. Wang¹, Z. H. Wang⁴², Z. Y. Wang¹, D. H. Wei¹⁰, J. B. Wei²⁸, P. Weidenkaff²⁰, S. P. Wen¹, M. Werner³⁷, U. Wiedner³, M. Wolke⁴⁶, L. H. Wu¹, N. Wu¹, Z. Wu¹, L. G. Xia³⁵, Y. Xia¹⁷, D. Xiao¹, Z. J. Xiao²⁵, Y. G. Xie¹, Q. L. Xiu¹, G. F. Xu¹, L. Xu¹, Q. J. Xu¹², Q. N. Xu³⁸, X. P. Xu³³, Z. Xue¹, L. Yan⁴², W. B. Yan⁴², W. C. Yan⁴², Y. H. Yan¹⁷, H. X. Yang¹, L. Yang⁴⁷, Y. Yang⁵, Y. X. Yang¹⁰, H. Ye¹, M. Ye¹, M. H. Ye⁶, B. X. Yu¹, C. X. Yu²⁷, H. W. Yu²⁸, J. S. Yu²³, S. P. Yu³⁰, C. Z. Yuan¹, W. L. Yuan²⁶, Y. Yuan¹, A. Yuncu^{36B}, A. A. Zafar⁴⁴, A. Zallo^{19A}, S. L. Zang²⁶, Y. Zeng¹⁷, B. X. Zhang¹, B. Y. Zhang¹, C. Zhang²⁶, C. B. Zhang¹⁷, C. C. Zhang¹, D. H. Zhang¹, H. H. Zhang³⁴, H. Y. Zhang¹, J. J. Zhang¹, J. Q. Zhang¹, J. W. Zhang¹, J. Y. Zhang¹, J. Z. Zhang¹, S. H. Zhang¹, X. J. Zhang¹, X. Y. Zhang³⁰, Y. Zhang¹, Y. H. Zhang¹, Z. H. Zhang⁵, Z. P. Zhang⁴², Z. Y. Zhang⁴⁷, G. Zhao¹, J. W. Zhao¹, Lei Zhao⁴², Ling Zhao¹, M. G. Zhao²⁷, Q. Zhao¹, Q. W. Zhao¹, S. J. Zhao⁴⁹, T. C. Zhao¹, X. H. Zhao²⁶, Y. B. Zhao¹, Z. G. Zhao⁴², A. Zhemchugov^{21,e}, B. Zheng⁴³, J. P. Zheng¹, Y. H. Zheng³⁸, B. Zhong²⁵, L. Zhou¹, Li Zhou²⁷, X. Zhou⁴⁷, X. K. Zhou³⁸, X. R. Zhou⁴², X. Y. Zhou¹, K. Zhu¹, K. J. Zhu¹, X. L. Zhu³⁵, Y. C. Zhu⁴², Y. S. Zhu¹, Z. A. Zhu¹, J. Zhuang¹, B. S. Zou¹, J. H. Zou¹

(BESIII Collaboration)

¹ Institute of High Energy Physics, Beijing 100049, People's Republic of China

² Beihang University, Beijing 100191, People's Republic of China

³ Bochum Ruhr-University, D-44780 Bochum, Germany

⁴ Carnegie Mellon University, Pittsburgh, Pennsylvania 15213, USA

⁵ Central China Normal University, Wuhan 430079, People's Republic of China

⁶ China Center of Advanced Science and Technology, Beijing 100190, People's Republic of China

⁷ COMSATS Institute of Information Technology, Lahore, Defence Road, Off Raiwind Road, 54000 Lahore, Pakistan

⁸ G.I. Budker Institute of Nuclear Physics SB RAS (BINP), Novosibirsk 630090, Russia

⁹ GSI Helmholtzcentre for Heavy Ion Research GmbH, D-64291 Darmstadt, Germany

¹⁰ Guangxi Normal University, Guilin 541004, People's Republic of China

¹¹ GuangXi University, Nanning 530004, People's Republic of China

¹² Hangzhou Normal University, Hangzhou 310036, People's Republic of China

- ¹³ *Helmholtz Institute Mainz, Johann-Joachim-Becher-Weg 45, D-55099 Mainz, Germany*
- ¹⁴ *Henan Normal University, Xinxiang 453007, People's Republic of China*
- ¹⁵ *Henan University of Science and Technology, Luoyang 471003, People's Republic of China*
- ¹⁶ *Huangshan College, Huangshan 245000, People's Republic of China*
- ¹⁷ *Hunan University, Changsha 410082, People's Republic of China*
- ¹⁸ *Indiana University, Bloomington, Indiana 47405, USA*
- ¹⁹ (A) *INFN Laboratori Nazionali di Frascati, I-00044, Frascati, Italy; (B) INFN and University of Perugia, I-06100, Perugia, Italy*
- ²⁰ *Johannes Gutenberg University of Mainz, Johann-Joachim-Becher-Weg 45, D-55099 Mainz, Germany*
- ²¹ *Joint Institute for Nuclear Research, 141980 Dubna, Moscow region, Russia*
- ²² *KVI, University of Groningen, NL-9747 AA Groningen, The Netherlands*
- ²³ *Lanzhou University, Lanzhou 730000, People's Republic of China*
- ²⁴ *Liaoning University, Shenyang 110036, People's Republic of China*
- ²⁵ *Nanjing Normal University, Nanjing 210023, People's Republic of China*
- ²⁶ *Nanjing University, Nanjing 210093, People's Republic of China*
- ²⁷ *Nankai University, Tianjin 300071, People's Republic of China*
- ²⁸ *Peking University, Beijing 100871, People's Republic of China*
- ²⁹ *Seoul National University, Seoul, 151-747 Korea*
- ³⁰ *Shandong University, Jinan 250100, People's Republic of China*
- ³¹ *Shanxi University, Taiyuan 030006, People's Republic of China*
- ³² *Sichuan University, Chengdu 610064, People's Republic of China*
- ³³ *Soochow University, Suzhou 215006, People's Republic of China*
- ³⁴ *Sun Yat-Sen University, Guangzhou 510275, People's Republic of China*
- ³⁵ *Tsinghua University, Beijing 100084, People's Republic of China*
- ³⁶ (A) *Ankara University, Dogol Caddesi, 06100 Tandogan, Ankara, Turkey; (B) Dogus University, 34722 Istanbul, Turkey; (C) Uludag University, 16059 Bursa, Turkey*
- ³⁷ *Universität Giessen, D-35392 Giessen, Germany*
- ³⁸ *University of Chinese Academy of Sciences, Beijing 100049, People's Republic of China*
- ³⁹ *University of Hawaii, Honolulu, Hawaii 96822, USA*
- ⁴⁰ *University of Minnesota, Minneapolis, Minnesota 55455, USA*
- ⁴¹ *University of Rochester, Rochester, New York 14627, USA*
- ⁴² *University of Science and Technology of China, Hefei 230026, People's Republic of China*
- ⁴³ *University of South China, Hengyang 421001, People's Republic of China*
- ⁴⁴ *University of the Punjab, Lahore-54590, Pakistan*
- ⁴⁵ (A) *University of Turin, I-10125, Turin, Italy; (B) University of Eastern Piedmont, I-15121, Alessandria, Italy; (C) INFN, I-10125, Turin, Italy*
- ⁴⁶ *Uppsala University, Box 516, SE-75120 Uppsala, Sweden*
- ⁴⁷ *Wuhan University, Wuhan 430072, People's Republic of China*
- ⁴⁸ *Zhejiang University, Hangzhou 310027, People's Republic of China*
- ⁴⁹ *Zhengzhou University, Zhengzhou 450001, People's Republic of China*
- ^a *Also at the Novosibirsk State University, Novosibirsk, 630090, Russia*
- ^b *Also at the Moscow Institute of Physics and Technology, Moscow 141700, Russia and at the Functional Electronics Laboratory, Tomsk State University, Tomsk, 634050, Russia*
- ^c *Also at University of Texas at Dallas, Richardson, Texas 75083, USA*
- ^d *Also at the PNPI, Gatchina 188300, Russia*
- ^e *Also at the Moscow Institute of Physics and Technology, Moscow 141700, Russia*

Abstract

Using 2917 pb^{-1} of data accumulated at 3.773 GeV , 44.5 pb^{-1} of data accumulated at 3.65 GeV and data accumulated during a $\psi(3770)$ line-shape scan with the BESIII detector, the reaction $e^+e^- \rightarrow p\bar{p}$ is studied considering a possible

interference between resonant and continuum amplitudes. The cross section of $e^+e^- \rightarrow \psi(3770) \rightarrow p\bar{p}$, $\sigma(e^+e^- \rightarrow \psi(3770) \rightarrow p\bar{p})$, is found to have two solutions, determined to be $(0.059_{-0.020}^{+0.070} \pm 0.012)$ pb with the phase angle $\phi = (255.8_{-26.6}^{+39.0} \pm 4.8)^\circ$ (< 0.166 pb at the 90% confidence level), or $\sigma(e^+e^- \rightarrow \psi(3770) \rightarrow p\bar{p}) = (2.57_{-0.13}^{+0.12} \pm 0.12)$ pb with $\phi = (266.9_{-6.3}^{+6.1} \pm 0.9)^\circ$ both of which agree with a destructive interference. Using the obtained cross section of $\psi(3770) \rightarrow p\bar{p}$, the cross section of $p\bar{p} \rightarrow \psi(3770)$, which is useful information for the future PANDA experiment, is estimated to be either $(9.8_{-3.9}^{+11.8})$ nb (< 27.5 nb at 90% C.L.) or $(425.6_{-43.7}^{+42.9})$ nb.

Keywords:

BESIII, charmonium decay, proton form factor

PACS: 13.20.Gd, 13.25.Gv, 13.40.Gp, 13.66.Bc, 14.20.Gh

1. Introduction

At e^+e^- colliders, charmonium states with $J^{PC} = 1^{--}$, such as the J/ψ , $\psi(3686)$, and $\psi(3770)$, are produced through electron-positron annihilation into a virtual photon. These charmonium states can then decay into light hadrons through either the three-gluon process ($e^+e^- \rightarrow \psi \rightarrow ggg \rightarrow \text{hadrons}$) or the one-photon process ($e^+e^- \rightarrow \psi \rightarrow \gamma^* \rightarrow \text{hadrons}$). In addition to the above two processes, the non-resonant process ($e^+e^- \rightarrow \gamma^* \rightarrow \text{hadrons}$) plays an important role, especially in the $\psi(3770)$ energy region where the non-resonant production cross section is comparable to the resonant one.

The $\psi(3770)$, the lowest lying 1^{--} charmonium state above the $D\bar{D}$ threshold, is expected to decay dominantly into the OZI-allowed $D\bar{D}$ final states [1, 2]. However, assuming no interference effects between resonant and non-resonant amplitudes, the BES Collaboration found a large total non- $D\bar{D}$ branching fraction of $(14.5 \pm 1.7 \pm 5.8)\%$ [3, 4, 5, 6]. A later work by the CLEO Collaboration, which included interference between one-photon resonant and one-photon non-resonant amplitudes (assuming no interference with the three-gluon amplitude), found a contradictory non- $D\bar{D}$ branching fraction of $(-3.3 \pm 1.4_{-4.8}^{+6.6})\%$ [7]. These different results could be caused by interference effects. Moreover, it has been noted that the interference of the non-resonant (continuum) amplitude with the three-gluon resonant amplitude should not be neglected [8]. To clarify the situation, many exclusive non- $D\bar{D}$ decays of the $\psi(3770)$ have been investigated [9, 10]. Low statistics, however, especially in the scan data sets have not permitted the inclusion of interference effects in these exclusive studies.

BESIII has collected the world's largest data sample of e^+e^- collisions at 3.773 GeV. Analyzed together with data samples taken during a $\psi(3770)$ line-shape scan, investigations of exclusive decays, taking into account the interference of resonant and non-resonant amplitudes are now possible. Recently, the decay channel of $\psi(3770) \rightarrow p\bar{p}\pi^0$ [11] has been studied considering the above mentioned interference. In this Letter, we report on a study of the two-body final state $e^+e^- \rightarrow p\bar{p}$ in the vicinity of the $\psi(3770)$ based on data sets collected with the upgraded Beijing Spectrometer (BESIII) located at the Beijing Electron-Positron Collider (BEPCII) [12]. The data sets include 2917 pb^{-1} of data at 3.773 GeV, 44.5 pb^{-1} of data at 3.65 GeV [13], and data taken during a $\psi(3770)$ line-shape scan in the energy range from 3.74 to 3.90 GeV.

2. BESIII detector

The BEPCII is a modern accelerator featuring a multi-bunch double ring and high luminosity, operating with beam energies between 1.0 and 2.3 GeV and a design luminosity of $1 \times 10^{33} \text{ cm}^{-2} \text{ s}^{-1}$. The BESIII detector is a high-performance general purpose detector. It is composed of a helium-gas based drift chamber (MDC) for charged-particle tracking and particle identification by specific ionization dE/dx , a plastic scintillator time-of-flight (TOF) system for additional particle identification, a CsI (TI) electromagnetic calorimeter (EMC) for electron identification and photon detection, a super-conducting solenoid magnet providing a 1.0 Tesla magnetic field, and a muon detector composed of resistive-plate chambers. The momentum resolution for charged particles at 1 GeV/c is 0.5%. The energy resolution of 1 GeV photons is 2.5%. More details on the accelerator and detector can be found in Ref. [12].

A GEANT4-based [14] Monte Carlo (MC) simulation software package, which includes a description of the geometry, material, and response of the BESIII detector, is used for detector simulations. The signal and background processes are generated with dedicated models that have been packaged and customized for BESIII [15]. Initial-state

radiation (ISR) effects are not included at the generator level for the efficiency determination, but are corrected later using a standard ISR correction procedure [16, 17]. In the ISR correction, PHOKHARA [18] is used to produce a MC-simulated sample of $e^+e^- \rightarrow \gamma_{\text{ISR}}p\bar{p}$ (without $\gamma_{\text{ISR}}J/\psi$ and $\gamma_{\text{ISR}}\psi(3686)$). For the estimation of backgrounds from $\gamma_{\text{ISR}}\psi(3686)$ and $e^+e^- \rightarrow \psi(3770) \rightarrow D\bar{D}$, MC-simulated samples with a size equivalent to 10 times the size of data samples are analyzed.

3. Event selection

The final state in this decay is characterized by one proton and one antiproton. Two charged tracks with opposite charge are required. Each track is required to have its point of closest approach to the beam axis within 10 cm of the interaction point in the beam direction and within 1 cm of the beam axis in the plane perpendicular to the beam. The polar angle of the track is required to be within the region $|\cos\theta| < 0.8$.

The TOF information is used to calculate particle identification (PID) probabilities for pion, kaon and proton hypotheses [19]. For each track, the particle type yielding the largest probability is assigned. Here, the momentum of proton is high ($> 1.6 \text{ GeV}/c$). For this high momentum protons and antiprotons, the PID efficiency is about 95%. The ratio of kaons to be mis-identified as protons is about 5%. In this analysis, one charged track is required to be identified as a proton and the other one as an antiproton.

The angle between the proton and antiproton ($\theta_{p\bar{p}}$) in the rest frame of the overall e^+e^- CMS system is required to be greater than 179 degrees. Finally, for both tracks, the absolute difference between the measured and the expected momentum (e.g. $1.637 \text{ GeV}/c$ for the $\psi(3770)$ data sample) should be less than $40 \text{ MeV}/c$ (about 3σ).

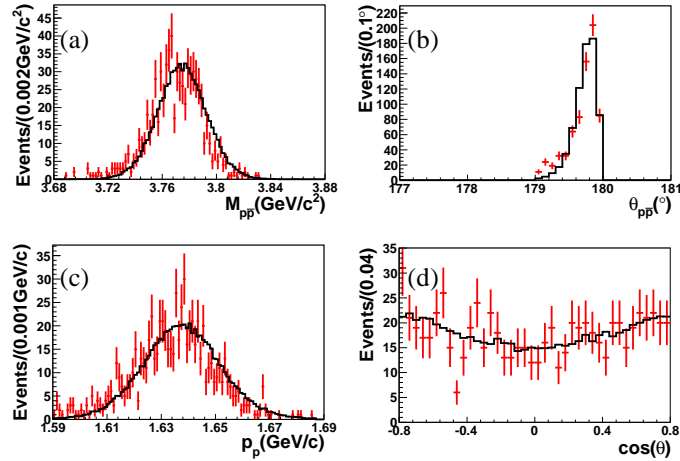


Figure 1: Comparisons between experimental and MC simulation data of selected $e^+e^- \rightarrow p\bar{p}$ events at 3.773 GeV. (a) The invariant mass of $p\bar{p}$ calculated with raw 4-momenta; (b) the angle between the proton and antiproton ($\theta_{p\bar{p}}$) in the rest frame of the overall e^+e^- CMS system; (c) the magnitude of the proton momentum; (d) the $\cos\theta$ of the proton momentum. The black histograms are MC simulations and the red crosses are experimental data.

After imposing the above event selection criteria, 684 ± 26 candidate events remain from the $\psi(3770)$ data set. Comparisons between experimental and MC data are plotted in Fig. 1. The MC simulation agrees with the experimental data. For other data sets, signal events are selected with similar selection criteria. Signal yields are listed in Table 1.

4. Background estimation

Background from ISR to the lower lying $\psi(3686)$ resonance, which is not taken into account in the ISR correction procedure, is estimated with a sample of MC-simulated data. The number of expected background events from this process is 0.1 and is neglected in this analysis.

Table 1: Summary of results at center-of-mass energies from 3.65 to 3.90 GeV. N_{sig} is the number of $e^+e^- \rightarrow p\bar{p}$ events; ϵ is the detection efficiency; L is the integrated luminosity; $(1 + \delta)_{dressed}$ is the initial state radiation correction factor without the vacuum polarization correction; and σ_{obs} , $\sigma_{dressed}$ and σ_{Born} are the observed cross section, the dressed cross section and the Born cross section, respectively.

$\sqrt{s}(\text{GeV})$	N_{sig}	$\epsilon(\%)$	$L(\text{pb}^{-1})$	$(1 + \delta)_{dressed}$	$\sigma_{obs}(\text{pb})$	$\sigma_{dressed}(\text{pb})$	$\sigma_{Born}(\text{pb})$
3.650	26.0 ± 5.1	62.6 ± 0.4	44.5	0.76	$0.90 \pm 0.18 \pm 0.06$	$1.19 \pm 0.24 \pm 0.08$	$1.12 \pm 0.22 \pm 0.08$
3.748	$1.0^{+1.8}_{-0.6}$	61.2 ± 0.4	3.57	0.76	$0.46^{+0.83}_{-0.28} \pm 0.03$	$0.60^{+1.08}_{-0.36} \pm 0.04$	$0.54^{+0.97}_{-0.32} \pm 0.04$
3.752	$3.0^{+2.3}_{-1.9}$	60.8 ± 0.4	6.05	0.76	$0.82^{+0.63}_{-0.52} \pm 0.06$	$1.07^{+0.82}_{-0.68} \pm 0.08$	$0.96^{+0.74}_{-0.61} \pm 0.07$
3.755	$4.0^{+2.8}_{-1.7}$	61.7 ± 0.4	7.01	0.77	$0.93^{+0.65}_{-0.39} \pm 0.06$	$1.21^{+0.85}_{-0.51} \pm 0.09$	$1.09^{+0.76}_{-0.46} \pm 0.08$
3.760	$4.0^{+2.8}_{-1.7}$	62.4 ± 0.4	8.65	0.77	$0.74^{+0.52}_{-0.32} \pm 0.05$	$0.96^{+0.67}_{-0.41} \pm 0.07$	$0.87^{+0.61}_{-0.37} \pm 0.06$
3.766	$0.0^{+1.3}_{-0.0}$	62.4 ± 0.4	5.57	0.79	$0.00^{+0.37}_{-0.00} (< 0.70)$	$0.00^{+0.47}_{-0.00} (< 0.89)$	$0.00^{+0.43}_{-0.00} (< 0.81)$
3.772	$0.0^{+1.3}_{-0.0}$	62.5 ± 0.4	3.68	0.80	$0.00^{+0.56}_{-0.00} (< 1.06)$	$0.00^{+0.70}_{-0.00} (< 1.33)$	$0.00^{+0.64}_{-0.00} (< 1.20)$
3.773	684 ± 26	62.3 ± 0.4	2917	0.80	$0.38 \pm 0.01 \pm 0.03$	$0.47 \pm 0.02 \pm 0.04$	$0.43 \pm 0.02 \pm 0.03$
3.778	$0.0^{+1.3}_{-0.0}$	62.6 ± 0.4	3.61	0.78	$0.00^{+0.57}_{-0.00} (< 1.08)$	$0.00^{+0.74}_{-0.00} (< 1.39)$	$0.00^{+0.66}_{-0.00} (< 1.25)$
3.784	$0.0^{+1.3}_{-0.0}$	62.4 ± 0.4	4.57	0.75	$0.00^{+0.45}_{-0.00} (< 0.85)$	$0.00^{+0.60}_{-0.00} (< 1.14)$	$0.00^{+0.54}_{-0.00} (< 1.02)$
3.791	$1.0^{+1.8}_{-0.6}$	62.1 ± 0.4	6.10	0.74	$0.26^{+0.48}_{-0.16} \pm 0.02$	$0.35^{+0.64}_{-0.21} \pm 0.02$	$0.32^{+0.57}_{-0.19} \pm 0.02$
3.798	$3.0^{+2.3}_{-1.9}$	61.9 ± 0.4	7.64	0.75	$0.63^{+0.49}_{-0.40} \pm 0.04$	$0.85^{+0.65}_{-0.54} \pm 0.06$	$0.77^{+0.59}_{-0.48} \pm 0.05$
3.805	$1.0^{+1.8}_{-0.6}$	61.5 ± 0.4	4.34	0.75	$0.37^{+0.67}_{-0.22} \pm 0.03$	$0.50^{+0.90}_{-0.30} \pm 0.04$	$0.45^{+0.81}_{-0.27} \pm 0.03$
3.810	20.0 ± 4.5	62.4 ± 0.4	52.60	0.75	$0.61 \pm 0.14 \pm 0.04$	$0.81 \pm 0.18 \pm 0.06$	$0.73 \pm 0.16 \pm 0.05$
3.819	$1.0^{+1.8}_{-0.6}$	61.4 ± 0.4	1.05	0.75	$1.55^{+2.79}_{-0.95} \pm 0.11$	$2.06^{+3.70}_{-1.23} \pm 0.14$	$1.85^{+3.34}_{-1.11} \pm 0.13$
3.900	$12.0^{+4.3}_{-3.2}$	61.7 ± 0.4	52.61	0.76	$0.37^{+0.13}_{-0.10} \pm 0.03$	$0.49^{+0.17}_{-0.13} \pm 0.03$	$0.44^{+0.16}_{-0.12} \pm 0.03$

Background from $\psi(3770) \rightarrow D\bar{D}$ is estimated with an inclusive MC sample and can also be neglected. Exclusive channels, such as $e^+e^- \rightarrow K^+K^-$, $\mu^+\mu^-$, $\tau^+\tau^-$, $p\bar{p}\pi^0$, $p\bar{p}\gamma$ are also studied. The total background contribution is estimated to be 0.4 events, which is equivalent to a contamination ratio of 0.06%. Contributions from decay channels with unmeasured branching fractions for the $\psi(3770)$ are estimated by the branching fractions of the corresponding decay channels of $\psi(3686)$. These background contributions from unmeasured decay modes are taken into account in the systematic uncertainty (0.06%) instead of being subtracted directly.

The data set at 3.65 GeV contains a contribution from the $\psi(3686)$ tail, whose cross section is estimated to be 0.136 ± 0.012 nb [6]. The normalized contribution from this tail, 0.89 events, is also statistically subtracted from the raw signal yield.

5. Determination of cross sections

The observed cross sections at the center-of-mass energies $\sqrt{s} = 3.65, 3.773$ GeV and the fourteen different energy points in the vicinity of the $\psi(3770)$ resonance are determined according to $\sigma = \frac{N_{sig}}{\epsilon L}$, where ϵ is the detection efficiency determined from MC simulation and L is the integrated luminosity for each energy point. The observed cross sections are listed in Table 1. For energy points with no significant signal, upper limits on the cross section at 90% C.L. are given using the Feldman-Cousins method from Ref. [20].

The observed cross section of $e^+e^- \rightarrow p\bar{p}$ contains the lowest order Born cross section and some higher order contributions. The BaBar Collaboration [21, 22] has taken into account bremsstrahlung, e^+e^- self-energy and vertex corrections in their radiative correction. Vacuum polarization is included in their reported cross section. This corrected cross section, which is the sum of the Born cross section and the contribution of vacuum polarization, is called the dressed cross section. In order to use the BaBar measurements of $\sigma(e^+e^- \rightarrow p\bar{p})$ [21, 22] in our investigation, a radiative correction is performed to calculate the dressed cross section using the method described in Refs. [16, 17]. With the observed cross sections as our initial input, a fit to the line-shape equation (Eq. (1)) is performed iteratively. At each iteration, the ISR correction factors are calculated and the dressed cross sections are updated. The calculation converges after a few iterations (~ 5). The dressed cross section at each data point is listed in Table 1. As a reference, the Born cross sections are also calculated and given in Table 1. The Born cross section around 3.773 GeV is in excellent agreement with a previous measurement obtained with CLEO data [23].

6. Fit to the cross section

To extract the $\psi(3770) \rightarrow p\bar{p}$ cross section, the total cross section as a function of \sqrt{s} is constructed and a fit to the measured values is performed. As discussed in the introduction, the measured cross section is composed of three contributions: the three-gluon resonant process (A_{3g}), the one-photon resonant process (A_γ) and the non-resonant process (A_{con}). For the exclusive light hadron decay of the $\psi(3770)$, the contribution of the electromagnetic process A_γ is negligible compared to that of the three-gluon strong interaction A_{3g} [24]. The resonant amplitude can then be written as $A_\psi \equiv A_{3g} + A_\gamma \sim A_{3g}$. Finally, the total cross section can be constructed with only two amplitudes, A_ψ and A_{con} ,

$$\begin{aligned}\sigma(s) &= |A_{con} + A_\psi e^{i\phi}|^2 \\ &= \left| \sqrt{\sigma_{con}(s)} + \sqrt{\sigma_\psi} \frac{m_\psi \Gamma_\psi}{s - m_\psi^2 + im_\psi \Gamma_\psi} e^{i\phi} \right|^2,\end{aligned}\quad (1)$$

where m_ψ and Γ_ψ are the mass and width of the $\psi(3770)$ [25], respectively; ϕ describes the phase angle between the continuum and resonant amplitudes, which is a free parameter to be determined in the fit; and σ_ψ is the resonant cross section, which is also a free parameter.

The continuum cross section, σ_{con} , has been measured by many experiments [21, 22, 26, 27]. In Ref. [26] from the BESII Collaboration, σ_{con} was measured from 2 to 3.07 GeV, and is well-described with an s dependence according to

$$\sigma_{con}(s) = \frac{4\pi\alpha^2 v}{3s} \left(1 + \frac{2m_p^2}{s} \right) |G(s)|^2, \quad (2)$$

$$|G(s)| = \frac{C}{s^2 \ln^2(s/\Lambda^2)}. \quad (3)$$

Here α is the fine-structure constant; m_p is the nominal proton mass; v is the proton velocity in the e^+e^- rest frame; $G(s)$ is the effective proton form factor [27]; $\Lambda = 0.3$ GeV is the QCD scale parameter; and C is a free parameter.

The dressed cross sections in Table 1, together with the BaBar measurements of the cross sections between 3 and 4 GeV, are fitted with Eq. (1). In this fit, 26 data points are considered: 16 points from this investigation by BESIII, 5 points from Ref. [21] and 5 points from Ref. [22]. The free parameters are the phase angle ϕ , the resonant cross section σ_ψ , and C from the form factor describing the contribution of the continuum. Fig. 2 shows the data points and the fit result.

The fit yields a χ^2/ndf of 13.4/23. Two solutions are found with the same χ^2 and the same parameter C of (62.0 ± 2.3) GeV⁴. Two solutions are found because the cross section in Eq. (1) is constructed with the square of two amplitudes. This multi-solution problem has been explained in Ref. [28]. A dip indicating destructive interference is seen clearly in the fit (the red solid line in Fig. 2). The first solution for the cross section is $\sigma_{dressed}(e^+e^- \rightarrow \psi(3770) \rightarrow p\bar{p}) = (0.059_{-0.020}^{+0.070})$ pb with a phase angle $\phi = (255.8_{-26.6}^{+39.0})^\circ$ (< 0.166 pb at the 90% C.L.). The second solution is $\sigma_{dressed}(e^+e^- \rightarrow \psi(3770) \rightarrow p\bar{p}) = (2.57_{-0.13}^{+0.12})$ pb with a phase angle $\phi = (266.9_{-6.3}^{+6.1})^\circ$.

For comparison, an alternative fit with only the BESIII data points is performed. Two solutions are found with the same χ^2/ndf of 6.8/13 and the same parameter C of (62.6 ± 4.1) GeV⁴. The first solution for the cross section is $\sigma_{dressed}(e^+e^- \rightarrow \psi(3770) \rightarrow p\bar{p}) = (0.067_{-0.034}^{+0.088})$ pb with a phase angle $\phi = (253.8_{-25.4}^{+40.7})^\circ$. The second solution is $\sigma_{dressed}(e^+e^- \rightarrow \psi(3770) \rightarrow p\bar{p}) = (2.59 \pm 0.20)$ pb with a phase angle $\phi = (266.4 \pm 6.3)^\circ$. These two solutions agree with those from the previous fit, but have larger uncertainties.

Table 2 shows a summary of the fit results, where the first error is from the fit and the second error is from the correlated systematic uncertainties.

7. Systematic uncertainty study

The sources of systematic uncertainty in the cross section measurements are divided into two categories: uncorrelated and correlated uncertainties between different energy points. The former includes only the statistical uncertainty in the MC simulated samples (0.4%), which can be directly considered in the fit. The latter refers to the uncertainties that are correlated among different energy points, such as the tracking (4% for two charged tracks), particle identification (4% for both proton and antiproton), and integrated luminosity. The integrated luminosity for the data was

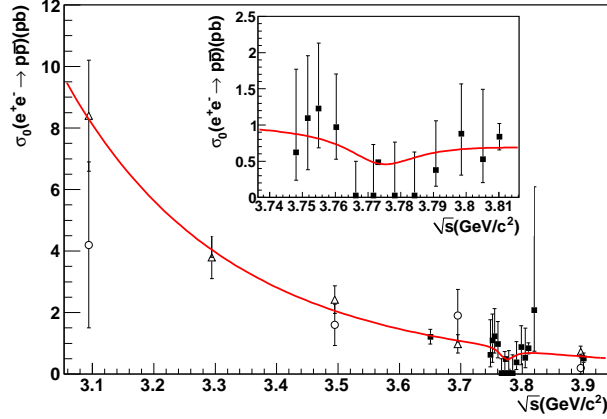


Figure 2: Fit to the dressed cross section of $e^+e^- \rightarrow p\bar{p}$ as a function of center-of-mass energy. The red dashed line shows the fit curve. The solid square points with error bars are from BESIII. The open circles are from the BaBar measurements of Ref. [21], and the open triangles from Ref. [22]. The inset shows a zoom of the region in the vicinity of the $\psi(3770)$.

Table 2: Summary of the extracted results for different solutions of the fit. Upper limits are determined at 90% C.L.

Solution	$\sigma_{(\psi(3770) \rightarrow p\bar{p})}^{dressed}$ (pb)	ϕ ($^\circ$)
(1)	$0.059^{+0.070}_{-0.020} \pm 0.012$ (< 0.166 at 90% C.L.)	$255.8^{+39.0}_{-26.6} \pm 4.8$
(2)	$2.57^{+0.12}_{-0.13} \pm 0.12$	$266.9^{+6.1}_{-6.3} \pm 0.9$

measured by analyzing large angle Bhabha scattering events [13] and has a total uncertainty of 1.1% at each energy point.

To estimate the uncertainty from the radiative corrections, a different correction procedure using the structure-function method [29] is applied, and the difference in results from these two correction procedures (2%) is taken as the uncertainty. To investigate the impact of the possible inconsistency of the MC simulation and experimental data, an alternative MC simulated sample is generated with a different proton momentum resolution (15% better than the previous MC sample), and the change in the final results (1.4%) is taken as the uncertainty.

In addition, the uncertainty on the reconstruction efficiency from the unmeasured angular distribution of the proton in the rest frame of the overall e^+e^- CMS system is also studied. According to hadron helicity conservation, the angular distribution of $\psi \rightarrow p\bar{p}$ can be expressed as $\frac{dN}{d\cos\theta} \propto 1 + \alpha \cos^2\theta$, where θ is the angle between the proton and the positron beam direction in the center-of-mass system. The theoretical value of $\alpha = 0.813$ [30] is used to produce the MC simulated sample in this analysis. In the case of $\psi(3686) \rightarrow p\bar{p}$, the mean value of α measured by E835 (0.67 ± 0.16) [31] differs by 0.13 from the theoretical value of 0.80. To obtain a conservative uncertainty, an alternative MC simulated sample with $\alpha = 0.683$ is used and the difference in the results (1.0%) is taken as the uncertainty. The uncertainty from the angle cut between the proton and antiproton is investigated by varying the angle cut (from 178.9 to 179.5 degrees) and the difference (2.2%) is taken as the uncertainty.

All of the above sources of uncertainty are applied to the observed cross section at each energy point. The total systematic uncertainty of the individual energy points is 6.7%.

The systematic uncertainties on the parameters extracted from the fit, such as $\sigma_{(\psi(3770) \rightarrow p\bar{p})}^{dressed}$ and the phase angle ϕ , are estimated by the ‘‘offset method’’ [32], in which the error propagation is determined from shifting the data by the aforementioned correlated uncertainties and adding the deviations in quadrature. In addition, a 1 MeV uncertainty for the beam energy measurements of all the data points is considered in the fit.

8. Summary and Discussion

Using 2917 pb⁻¹ of data collected at 3.773 GeV, 44.5 pb⁻¹ of data collected at 3.65 GeV and data collected during a $\psi(3770)$ line-shape scan with the BESIII detector, the reaction $e^+e^- \rightarrow p\bar{p}$ has been studied. To extract the cross section of $e^+e^- \rightarrow \psi(3770) \rightarrow p\bar{p}$, a fit, taking into account the interference of resonant and continuum amplitudes, is performed. In this investigation, the measured cross sections of $e^+e^- \rightarrow p\bar{p}$ from the BaBar experiment are included in a simultaneous fit to put more constraints on the continuum amplitude. The dressed cross section of $e^+e^- \rightarrow \psi(3770) \rightarrow p\bar{p}$ is extracted from the fit and shown in Table 2.

With the obtained dressed cross section of $e^+e^- \rightarrow \psi(3770) \rightarrow p\bar{p}$, the branching fraction $B_{\psi(3770) \rightarrow p\bar{p}}$ is determined to be $(7.1^{+8.6}_{-2.9}) \times 10^{-6}$ or $(3.1 \pm 0.3) \times 10^{-4}$, by dividing the dressed cross section of $e^+e^- \rightarrow \psi(3770)$ [7]. Even the larger solution has a relatively small branching fraction comparing to the large total non- $D\bar{D}$ branching fraction. Thus, the $p\bar{p}$ channel alone cannot explain the large non- $D\bar{D}$ branching fraction from BESII.

Using the branching fraction of $\psi(3770) \rightarrow p\bar{p}$, the cross section of its time reversed reaction $p\bar{p} \rightarrow \psi(3770)$ can be estimated using the Breit-Wigner formula [25]:

$$\sigma_{p\bar{p} \rightarrow \psi(3770)}(s) = \frac{4\pi(2J+1)}{(s-4m_p^2)} \frac{B_{\psi(3770) \rightarrow p\bar{p}}}{1 + [2(\sqrt{s} - M_\psi)/\Gamma_\psi]^2} \quad (4)$$

where M_ψ and Γ_ψ are the mass and width of the $\psi(3770)$ resonance, J is the spin of the $\psi(3770)$, and m_p is the proton mass. For the condition $\sqrt{s} = M_\psi$, the cross section $\sigma(p\bar{p} \rightarrow \psi(3770))$ is estimated to be either $(9.8^{+11.8}_{-3.9})$ nb (< 27.5 nb at 90% C.L.) or $(425.6^{+42.9}_{-43.7})$ nb.

The future PANDA (anti-Proton ANnihilations at DArmstadt) experiment is one of the key projects at the Facility for Antiproton and Ion Research (FAIR), which is currently under construction at GSI, Darmstadt. It will perform precise studies of antiproton-proton annihilations with various internal proton or nuclear targets and an anti-proton beam in the momentum range from 1.5 GeV/c to 15 GeV/c. In PANDA, a detailed investigation of the charmonium spectrum and the open charm channels is foreseen. For this physics program, it is important to obtain experimental information on the so far unknown open charm cross sections, both to evaluate luminosity requirements and to design detector. Theoretical estimations vary with several orders of magnitude [33, 34, 35, 36, 37, 38, 39, 40, 41]. In the physics performance report for PANDA [42], the $D\bar{D}$ production cross section is estimated to be 6.35 nb, with the unknown branching ratio of $\psi(3770) \rightarrow p\bar{p}$ scaled from the known ratio of $J/\psi \rightarrow p\bar{p}$. In this paper, the cross section of $\sigma(p\bar{p} \rightarrow \psi(3770))$ has been determined. As the first charmonium state above the $D\bar{D}$ threshold, $\psi(3770)$ could be used as a source of open charm production.

In this paper, two solutions on the cross section of $\sigma(p\bar{p} \rightarrow \psi(3770))$ are obtained. It is impossible to distinguish these two solutions with our data. The first solution, $(9.8^{+11.8}_{-3.9})$ nb, is compatible with a simple scaling from J/ψ used in the PANDA physics performance report. The second solution, with the cross section of $(425.6^{+42.9}_{-43.7})$ nb, is two order of magnitudes larger.

9. Acknowledgement

The BESIII collaboration thanks the staff of BEPCII and the computing center for their strong support. This work is supported in part by the Ministry of Science and Technology of China under Contract No. 2009CB825200; Joint Funds of the National Natural Science Foundation of China under Contracts Nos. 11079008, 11179007, U1332201; National Natural Science Foundation of China (NSFC) under Contracts Nos. 10625524, 10821063, 10825524, 10835001, 10935007, 11125525, 11235011; the Chinese Academy of Sciences (CAS) Large-Scale Scientific Facility Program; CAS under Contracts Nos. KJCX2-YW-N29, KJCX2-YW-N45; 100 Talents Program of CAS; German Research Foundation DFG under Contract No. Collaborative Research Center CRC-1044; Istituto Nazionale di Fisica Nucleare, Italy; Ministry of Development of Turkey under Contract No. DPT2006K-120470; U. S. Department of Energy under Contracts Nos. DE-FG02-04ER41291, DE-FG02-05ER41374, DE-FG02-94ER40823, DESC0010118; U.S. National Science Foundation; University of Groningen (RuG) and the Helmholtzzentrum fuer Schwerionenforschung GmbH (GSI), Darmstadt; WCU Program of National Research Foundation of Korea under Contract No. R32-2008-000-10155-0.

References

- [1] P. A. Rapidis *et al.*, Phys. Rev. Lett. **39** (1978) 526.
- [2] W. Bacino *et al.*, Phys. Rev. Lett. **40** (1978) 671 .
- [3] M. Ablikim *et al.* [BES Collaboration], Phys. Lett. B **641** (2006) 145.
- [4] M. Ablikim *et al.* [BES Collaboration], Phys. Rev. Lett. **97** (2006) 121801.
- [5] M. Ablikim *et al.* [BES Collaboration], Phys. Lett. B **659** (2007) 74.
- [6] M. Ablikim *et al.* [BES Collaboration], Phys. Rev. D **76** (2007) 122002.
- [7] D. Besson *et al.* [CLEO Collaboration], Phys. Rev. Lett. **96** (2006) 092002.
- [8] P. Wang, C. Yuan, X. Mo, and D. Zhang, hep-ph/0212139 (2002).
- [9] M. Ablikim *et al.* [BESIII Collaboration], Phys. Rev. D **87** (2013) 112011.
- [10] G. S. Adams *et al.* [CLEO Collaboration], Phys. Rev. D **73** (2006) 012002.
- [11] M. Ablikim *et al.* [BESIII Collaboration], arXiv:1406.2486 [hep-ex] (2014).
- [12] M. Ablikim *et al.* [BESIII Collaboration], Nucl. Instrum. Meth. A **614** (2010) 345.
- [13] M. Ablikim *et al.* [BESIII Collaboration], Chinese Physics C **37** (2013) 123001.
- [14] S. Agostinelli *et al.* [GEANT4 Collaboration], Nucl. Instrum. Meth. A **506** (2003) 250.
- [15] R. G. Ping, Chinese Physics C **32** (2008) 599.
- [16] H. Hu, X. Qi, G. Huang, and Z. Zhao, High Energy Physics and Nuclear Physics **25** (2001) 701.
- [17] C. Edwards *et al.*, SLAC-PUB-5160 (1990).
- [18] H. Czyz *et al.*, Eur. Phys. J. C **35** (2004) 527.
- [19] M. Ablikim *et al.* [BESIII Collaboration], Phys. Rev. D **86** (2012) 032014.
- [20] G. J. Feldman and R. D. Cousins, Phys. Rev. D **57** (1998) 3873.
- [21] J. P. Lees *et al.* [BABAR Collaboration], Phys. Rev. D **87** (2013) 092005.
- [22] J. P. Lees *et al.* [BABAR Collaboration], Phys. Rev. D **88** (2013) 072009.
- [23] Kamal K. Seth *et al.*, Phys. Rev. Lett. **110** (2013) 022002.
- [24] P. Wang, X. H. Mo, and C. Z. Yuan, International Journal of Modern Physics A **21** (2006) 5163.
- [25] J. Beringer *et al.* [Particle Data Group], Phys. Rev. D **86** (2012) 010001.
- [26] M. Ablikim *et al.* [BES Collaboration], Phys. Lett. B **630** (2005) 14.
- [27] B. Aubert *et al.* [BABAR Collaboration], Phys. Rev. D **73** (2006) 012005.
- [28] K. Zhu *et al.*, Int. J. Mod. Phys. A **26** (2011) 4511.
- [29] E. A. Kuraev and V. S. Fadin, Sov. J. Nucl. Phys **41** (1985) 779.
- [30] C. Carimalo, Int. J. Mod. Phys. A **2** (1987) 249.
- [31] M. Ambrogiani *et al.* [Fermilab E835 Collaboration], Phys. Lett. B **610** (2005) 177.
- [32] M. Botje, Journal of Physics G: Nuclear and Particle Physics **28** (2002) 779.
- [33] A. Khodjamirian, C. Klein, Th. Mannel, and Y.M. Wang, Eur. Phys. J. A **48** (2012) 31.
- [34] A. I. Titov and B. Kampfer, Phys. Rev. C **78** (2008) 025201.
- [35] A. I. Titov and B. Kampfer, arXiv:1105.3847 [hep-ph].
- [36] P. Kroll, B. Quadder and W. Schweiger, Nucl. Phys. B **316** (1989) 373.
- [37] A. T. Goritschnig, P. Kroll and W. Schweiger, Eur. Phys. J. A **42** (2009) 43.
- [38] E. Braaten and P. Artoisenet, Phys. Rev. D **79** (2009) 114005.
- [39] J. Haidenbauer and G. Krein, Phys. Lett. B **687** (2010) 314.
- [40] J. Haidenbauer and G. Krein, Few Body Syst. **50** (2011) 183.
- [41] B. Kerbikov and D. Kharzeev, Phys. Rev. D **51** (1995) 6103.
- [42] M. F. M. Lutz *et al.* [PANDA Collaboration], arXiv:0903.3905v1 [hep-ex] (2009).